

Supporting Information for:

Synthesis, Modular Composition, and Electrochemical Properties of Lamellar Iron Sulfides

Noah E. Horwitz,^a Elena V. Shevchenko,^b Jehee Park,^c Eungje Lee,^c Jiaze Xie,^a Baorui Chen,^a Yu Zhong,^a Alexander S. Filatov,^a John S. Anderson^{*,a}

^aDepartment of Chemistry, University of Chicago, Chicago, Illinois 60637, United States

^bCenter for Nanoscale Materials, Argonne National Laboratory, Argonne, Illinois 60439, United States

^cChemical Sciences and Engineering Division, Argonne National Laboratory, Argonne, Illinois 60439, United States

Correspondence to: jsanderson@uchicago.edu

Table of Contents

Additional Synthetic Procedures.....	4
1-Li, Method 3	4
1-Li, Method 4 (to prepare films for UV-visible-NIR spectroscopy).....	4
1-Na.....	4
1-K	4
1-TMA	4
NMR Spectra	5
Figure S1: ^1H NMR spectrum of Fe(DEDTC) ₃ in CDCl ₃	5
Figure S2: ^1H NMR spectrum of Fe(EX) ₃ in CDCl ₃	6
Scanning Electron Microscopy	7
Figure S3. Representative SEM images of aggregates (a-b) and an isolated flake (d) of 1-Li. .	7
X-ray Powder Diffraction Measurements	8
Figure S4: XRPD patterns of materials synthesized from Fe(EX) ₃ with different salt additives (all measured wet as suspensions in DMF).	8
Figure S5: XRPD patterns of 1-TMA wet with DMF and dried.	8
X-ray Fluorescence Data.....	9
Figure S6: Representative XRF spectrum of 1-Li.	9
X-ray Absorption (XAS) Data and Fits	9
Figure S7: Comparison of Fe K-edge XANES (first derivative) from 1-Li to literature data for mackinawite and greigite.	9
Figure S8: EXAFS data from 1-Li (wet in DMF) with fit to mackinawite model presented in k-space.	10
Figure S9: EXAFS data from 1-Li (wet in DMF) with a) R-space and b) k-space fits to smythite model.....	10
Figure S10. EXAFS data from 1-Li (wet in DMF) with a) R-space and b) k-space fits to Li ₂ FeS ₂ model.	11
Table S1: EXAFS fitting parameters for 1-Li (wet in DMF) using structural models from mackinawite, smythite, and Li ₂ FeS ₂ crystal structures.....	12
Figure S11: Comparison of EXAFS data from wet (DMF) and dry samples of 1-Li in a) R- space and b) k-space.	12
Thermogravimetric Analysis (TGA).....	13
Figure S12: Thermogravimetric analysis data for three batches of 1-Li	13
UV-visible-NIR Spectroscopy	14
Figure S13: UV-visible-NIR absorption data for 1-Li.....	14
Variable-Temperature Electrical Conductivity.....	15

Figure S14: Relative electrical conductivity vs. temperature for a pressed pellet of 1-Li.	15
Figure S15: Linear fit to high temperature region of the variable temperature electrical conductivity plot shown in Figure S14.	16
Mössbauer Spectroscopy	17
Figure S16: ^{57}Fe Mössbauer spectrum of 1-Li collected at 80 K with fit to a two site model.	17
Table S2: Mössbauer fitting parameters.	17
IR Spectroscopy.....	18
Figure S17: FTIR spectrum of 1-Li prepared as a KBr pellet.	18
Electrochemical Measurements	18
Figure S18. Cyclic voltammograms (1 mV/s, 0.1 M LiCF_3SO_3 in DMF) of carbon paper electrode coated with 1-Li + 10% rubber slurry and control electrodes. Current densities are calculated using the geometric areas of the electrodes (2 cm^2).	18
Figure S19: Cyclic voltammetry data for 1-Li composite electrode in 0.1 M LiCF_3SO_3 /DMF showing Faradaic features.	19
Figure S20: Cyclic voltammograms of the same 1-Li composite electrode in different electrolytes, measured at 10 mV/s.	19
Figure S21: dQ/dV plot for 1-Li lithium ion cathode half cell tests at 0.1C.	20
Figure S22: Charge/discharge curves for 1-Li sodium ion cathode half cell tests.	20
Figure S23: dQ/dV plot for 1-Li sodium ion cathode half cell tests.....	21
Figure S24: Cycling stability of 1-Li sodium ion cathode in half cell tests.	21

Additional Synthetic Procedures

1-Li, Method 3

Fe(DEDTC)₃ (25 mg, 0.05 mmol) and LiCF₃SO₃ (39 mg, 0.25 mmol) were added to a vial and dissolved in DMF (2.5 mL). In a separate vial, dithio-p-urazine (15 mg, 0.1 mmol) was dissolved in DMF (2.5 mL). The solutions were combined and heated in a sealed vial to 100 °C for 24 h. The resulting black solid was isolated via centrifugation, washed 2x with DMF (2 mL) and 3x with THF (2 mL) to obtain **1-Li** (~7 mg, quant.).

1-Li, Method 4 (to prepare films for UV-visible-NIR spectroscopy)

Fe(EX)₃ (17 mg, 0.04 mmol) and LiCF₃SO₃ (31 mg, 0.2 mmol), and DMF (4 mL) were mixed and the resulting solution divided between two 4 mL vials. A sapphire substrate was added to each vial and the vials were maintained at room temperature for 2 days. During this time, a film of dark solid formed on the vial walls and the surfaces of the substrates. The substrates were washed 2x with DMF (2 mL) and 2x with THF (2 mL) before being dried under vacuum.

1-Na

Fe(DEDTC)₃ (25 mg, 0.05 mmol) and NaCF₃SO₃ (43 mg, 0.25 mmol) were added to a vial along with DMF (5 mL). The vial was sealed and shaken to dissolve all solids, then heated to 140 °C for 3 days. The resulting black solid was isolated via centrifugation, washed 2x with DMF (2 mL) and 3x with THF (2 mL) to obtain **1-Na**.

1-K

Fe(DEDTC)₃ (25 mg, 0.05 mmol) and KCF₃SO₃ (47 mg, 0.05 mmol) were added to a vial along with DMF (5 mL). The vial was sealed and shaken to dissolve all solids, then heated to 140 °C for 3 days. The resulting black solid was isolated via centrifugation, washed 2x with DMF (2 mL) and 3x with THF (2 mL) to obtain **1-K**.

1-TMA

Fe(DEDTC)₃ (25 mg, 0.05 mmol) and TMAPF₆ (55 mg, 0.05 mmol) were added to a vial along with DMF (5 mL). The vial was sealed and shaken to dissolve all solids, then heated to 140 °C for 3 days. The resulting black solid was isolated via centrifugation, washed 2x with DMF (2 mL) and 3x with THF (2 mL) to obtain **1-TMA**.

NMR Spectra

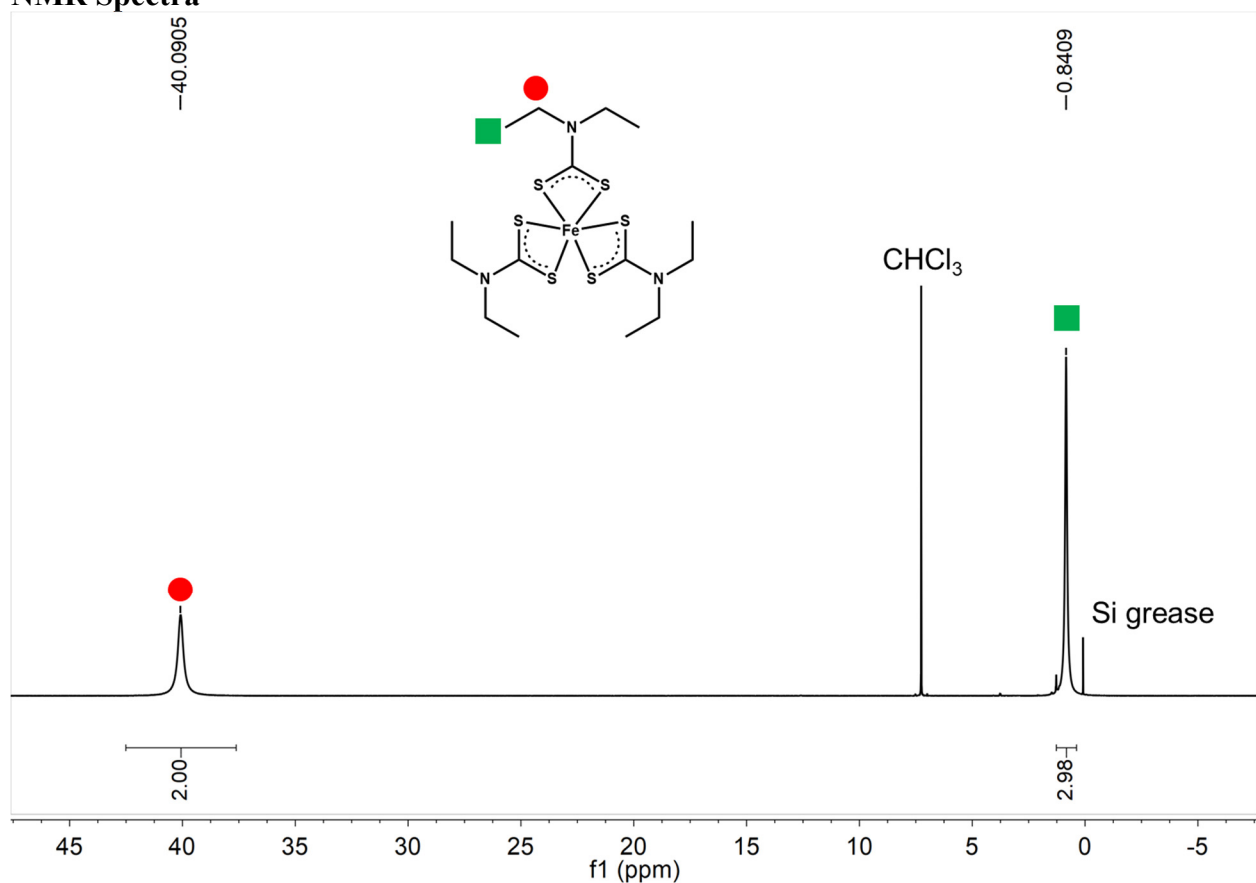


Figure S1: ^1H NMR spectrum of $\text{Fe}(\text{DEDTC})_3$ in CDCl_3 .

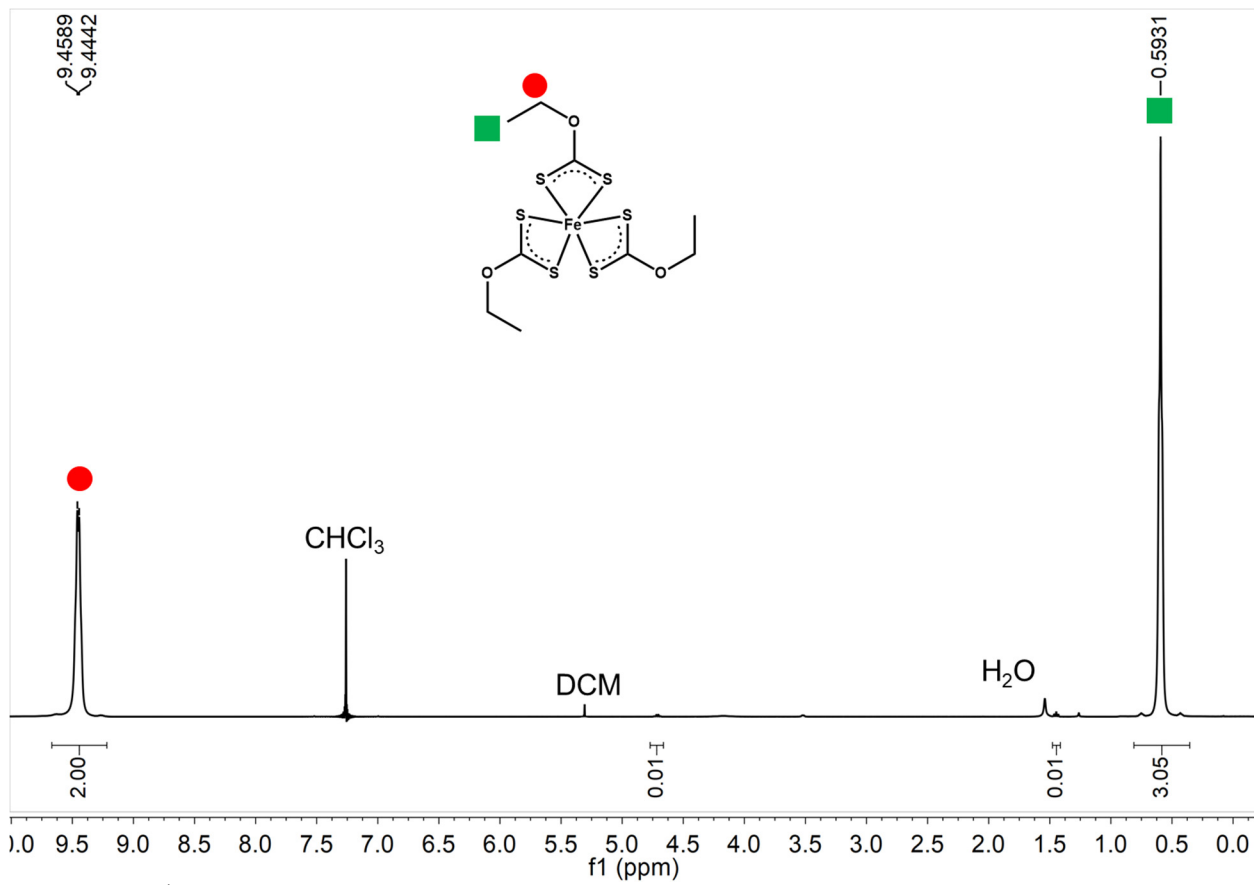


Figure S2: ^1H NMR spectrum of $\text{Fe}(\text{EX})_3$ in CDCl_3 . Small unlabeled peaks are due to traces of free ligand and methanol.

Scanning Electron Microscopy

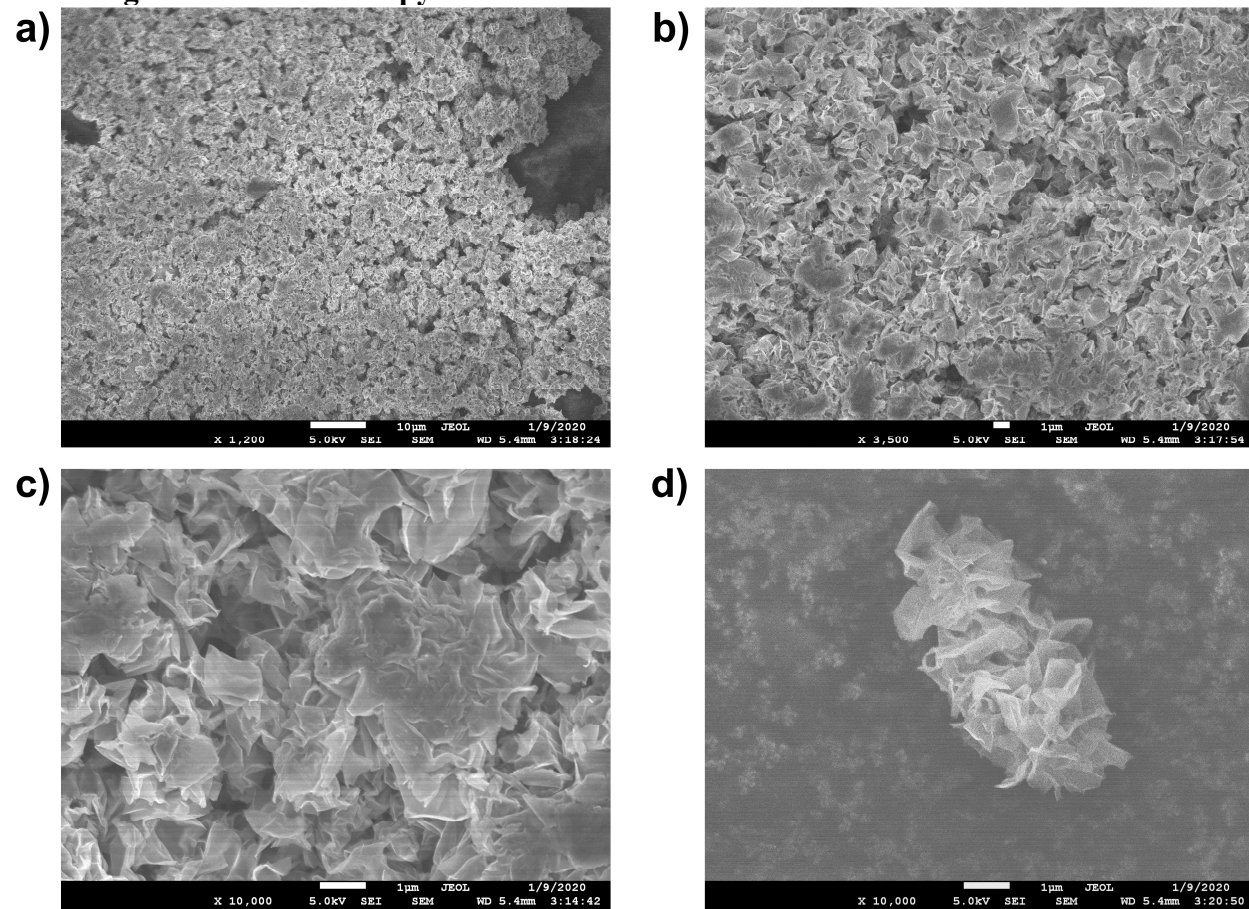


Figure S3. Representative SEM images of aggregates (a-b) and an isolated flake (d) of **1-Li**.

X-ray Powder Diffraction Measurements

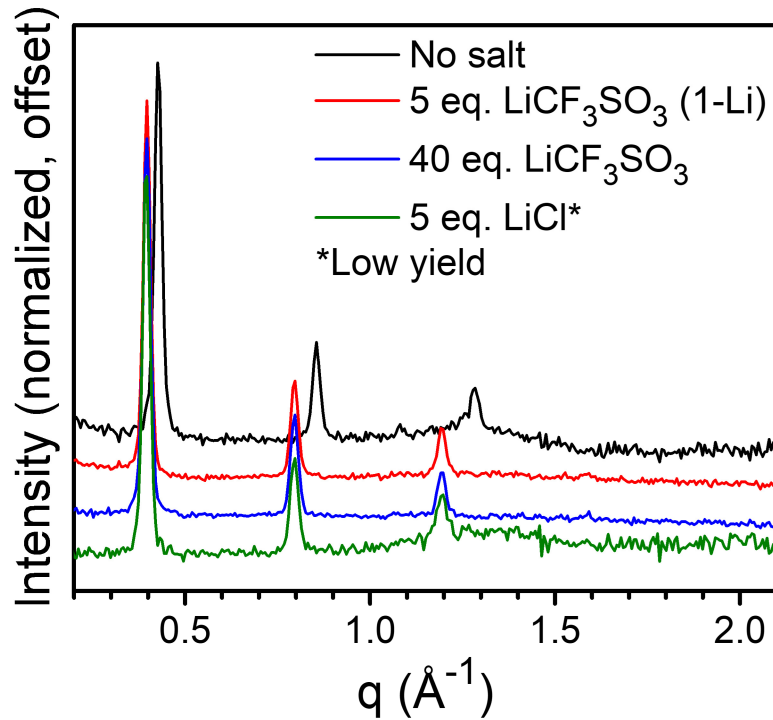


Figure S4: XRPD patterns of materials synthesized from $\text{Fe}(\text{EX})_3$ with different salt additives (all measured wet as suspensions in DMF).

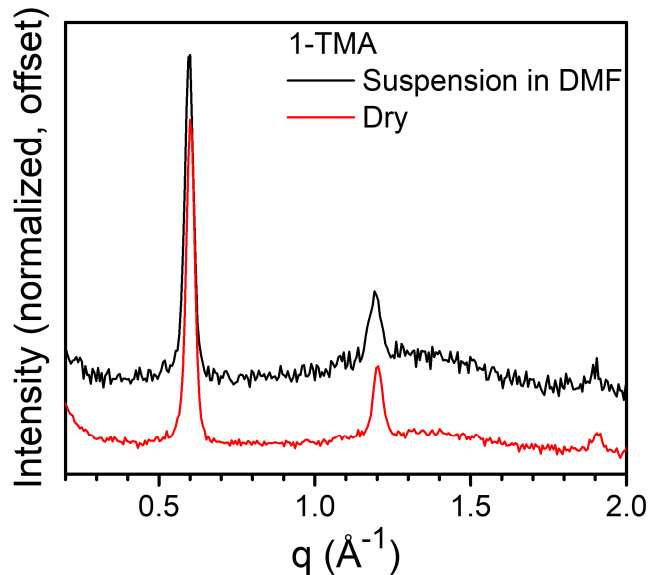


Figure S5: XRPD patterns of 1-TMA wet with DMF and dried.

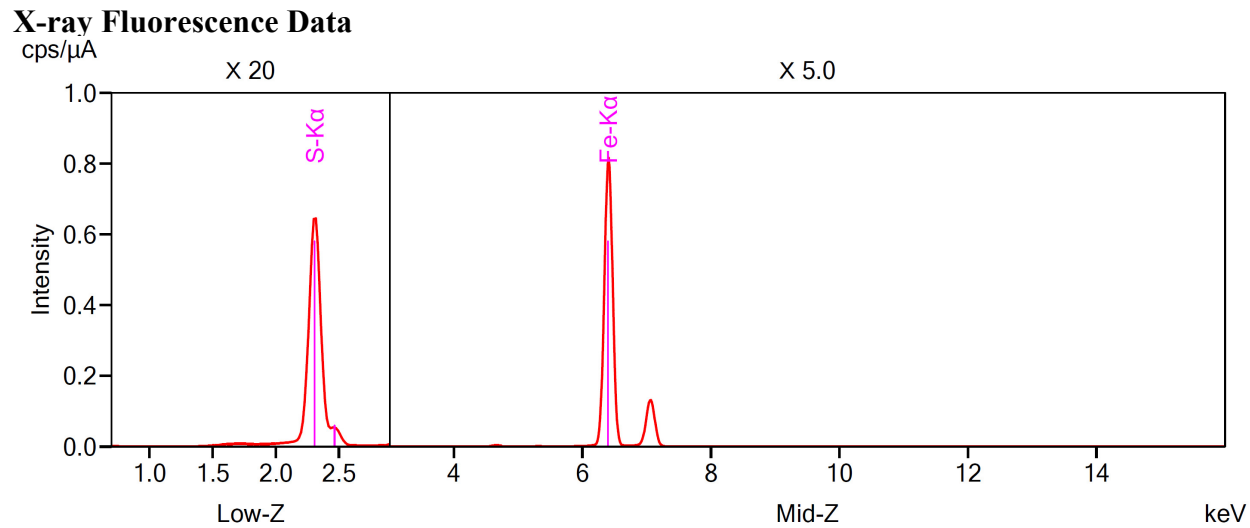


Figure S6: Representative XRF spectrum of **1-Li**.

X-ray Absorption (XAS) Data and Fits

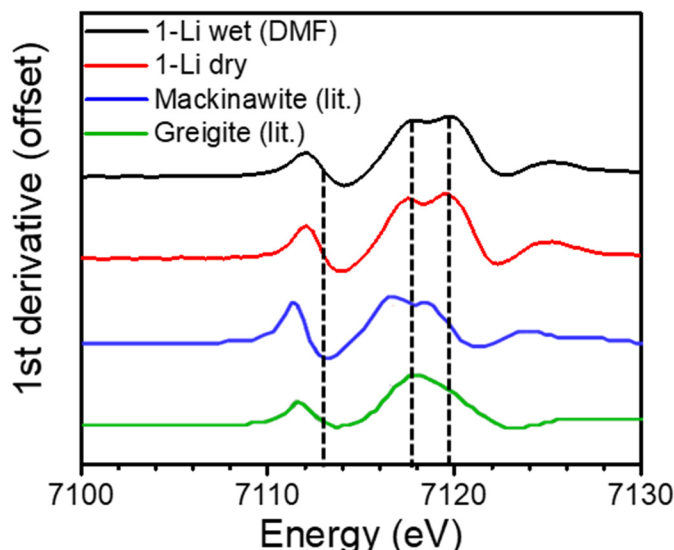


Figure S7: Comparison of Fe K-edge XANES (first derivative) from **1-Li** to literature data for mackinawite and greigite. Literature spectra adapted from Jeong et al., *Water Res.* **2013**, *47*, 6639-6649.

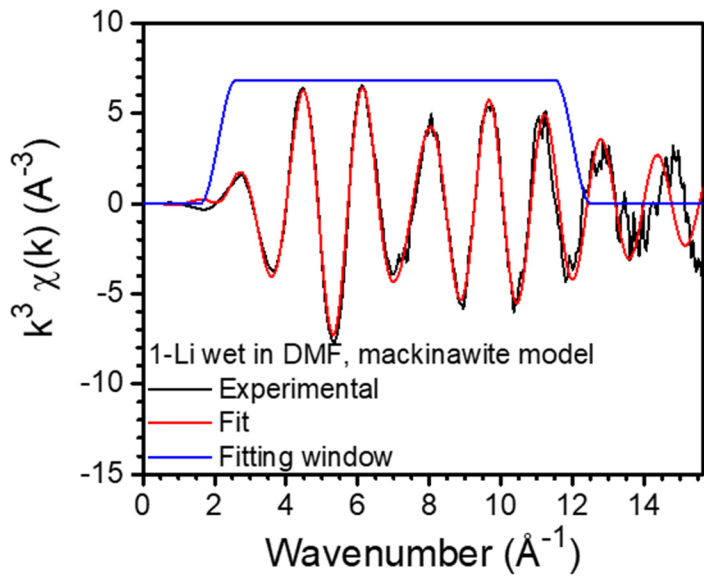


Figure S8: EXAFS data from **1-Li** (wet in DMF) with fit to mackinawite model presented in k-space.

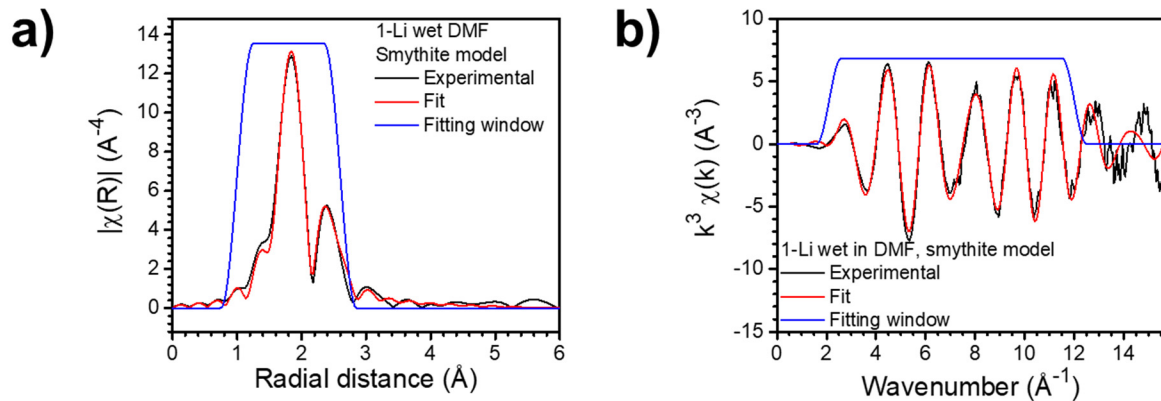


Figure S9: EXAFS data from **1-Li** (wet in DMF) with a) R-space and b) k-space fits to smythite model.

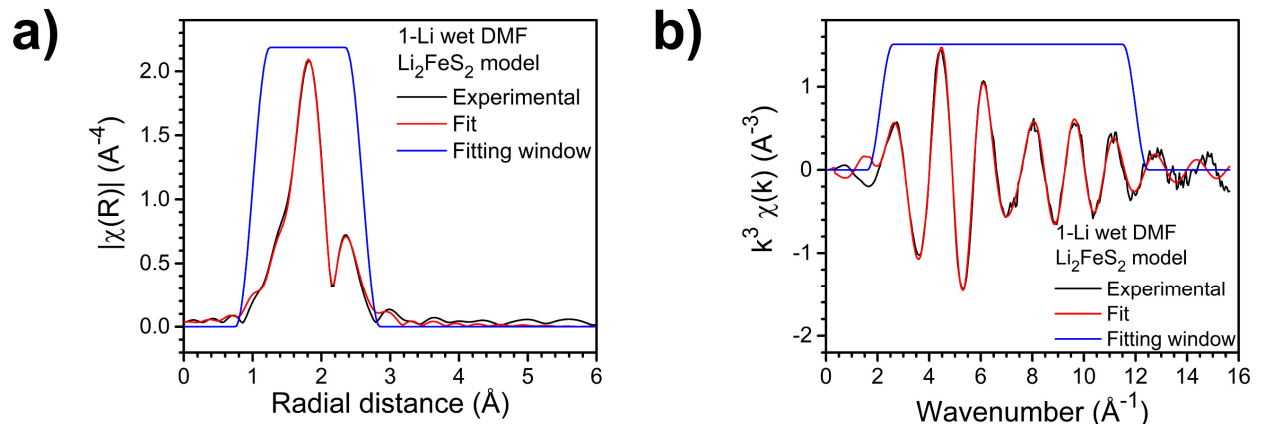


Figure S10. EXAFS data from 1-Li (wet in DMF) with a) R-space and b) k-space fits to Li_2FeS_2 model.

Table S1: EXAFS fitting parameters for **1-Li** (wet in DMF) using structural models from mackinawite, smythite, and Li_2FeS_2 crystal structures.

Mackinawite model	N	R (\AA)	$\sigma_2 (\text{\AA}^2)$	R-factor	Reduced chi-square
Fe ₁ -S	4	2.257(6)	0.0028(8)		
Fe ₁ -Fe ₂	4	2.71(2)	0.012(2)	0.0079	484
Independent points = 9.8, number of variables = 6, $\Delta E_0 = 1.3(7) \text{ eV}$, $S_0^2 = 0.67(5)$, fitting range $k = 2.1\text{-}12 \text{ \AA}^{-1}$ and $R = 1\text{-}2.6 \text{ \AA}$, k weights = 1, 2, 3					
Smythite model					
Fe ₁ -S	6	2.265(8)	0.004(1)		
Fe ₁ -Fe ₂	2	2.72(2)	0.003(2)	0.0097	802
Independent points = 9.8, number of variables = 6, $\Delta E_0 = 1.6(8) \text{ eV}$, $S_0^2 = 0.50(4)$, fitting range $k = 2.1\text{-}12 \text{ \AA}^{-1}$ and $R = 1\text{-}2.6 \text{ \AA}$, k weights = 1, 2, 3					
Li_2FeS_2 model					
Fe ₁ -S ₁	3	2.26(1)	0.0040(9)		
Fe ₁ -S ₂	1	2.67(6)	0.01(1)	0.0022	
Fe ₁ -Fe ₂	3	2.73(1)	0.010(3)		286
Independent points = 9.8, number of variables = 8, $\Delta E_0 = 0(1) \text{ eV}$, $S_0^2 = 1.03(9)$, fitting range $k = 2.1\text{-}12 \text{ \AA}^{-1}$ and $R = 1\text{-}2.6 \text{ \AA}$, k weights = 1, 2, 3					

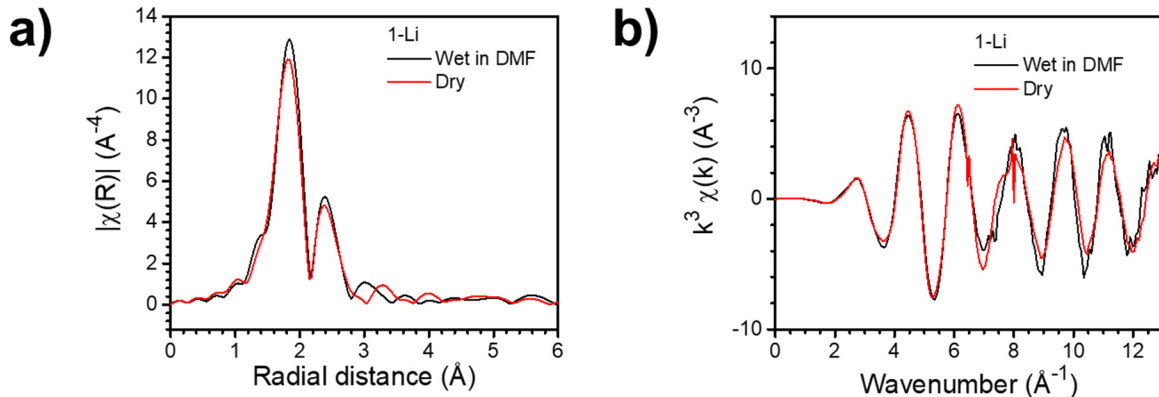


Figure S11: Comparison of EXAFS data from wet (DMF) and dry samples of **1-Li** in a) R-space and b) k-space.

Thermogravimetric Analysis (TGA)

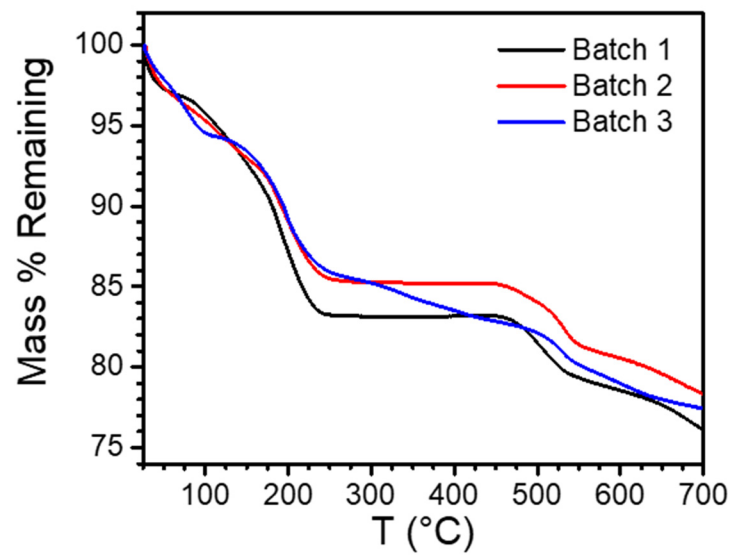


Figure S12: Thermogravimetric analysis data for three batches of **1-Li**, measured under N₂ with a 5 °C/min ramp rate.

UV-visible-NIR Spectroscopy

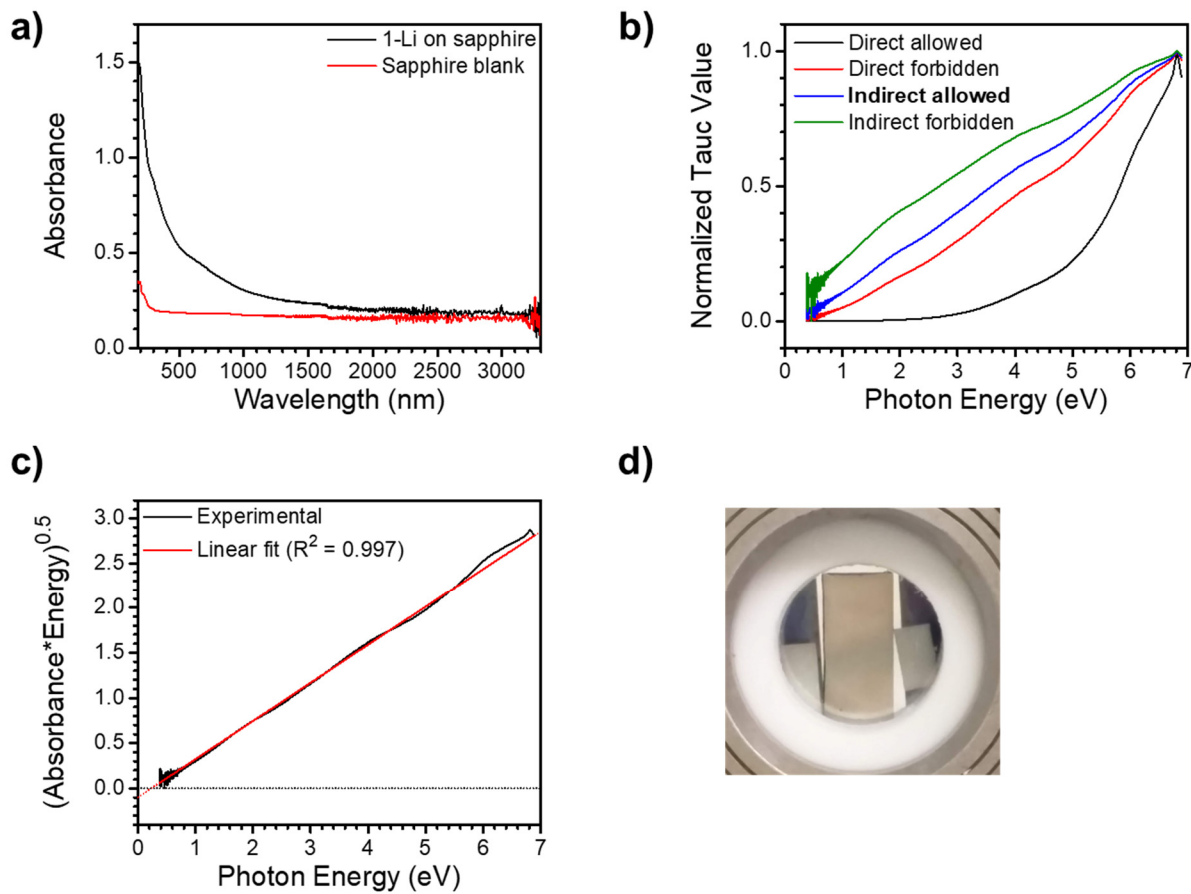


Figure S13: UV-visible-NIR absorption data for **1-Li**. a) UV-visible-NIR absorption spectrum of **1-Li** on sapphire (0001) and sapphire blank. b) Comparison of Tauc plots assuming different types of transitions. The indirect allowed transition produces the most linear plot. c) Tauc plot for indirect allowed transition with linear fit corresponding to $E_g = 0.23$ eV. Dotted lines highlight the X-axis and the linear fit as a visual guide. d) Photograph of **1-Li** on sapphire (0001) sample (center) in holder.

Variable-Temperature Electrical Conductivity

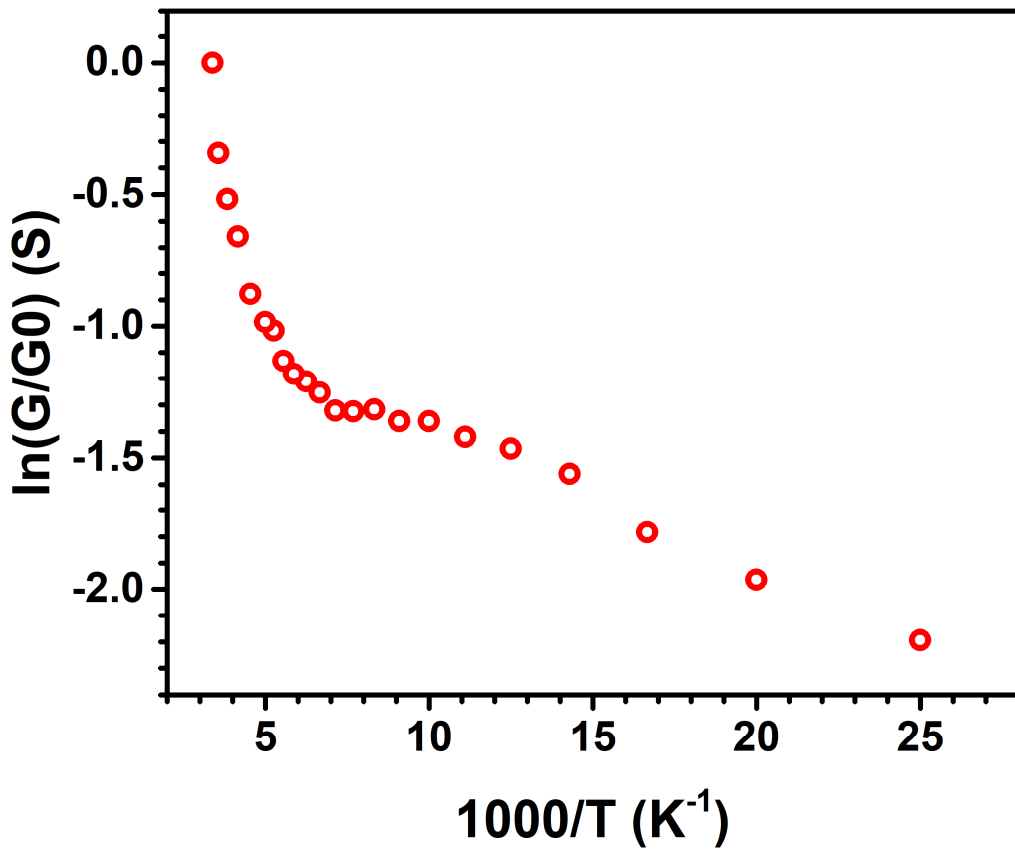


Figure S14: Relative electrical conductivity vs. temperature for a pressed pellet of **1-Li**. The presence of two linear regions and a plateau near 100 K may indicate a phase transition at low temperatures.

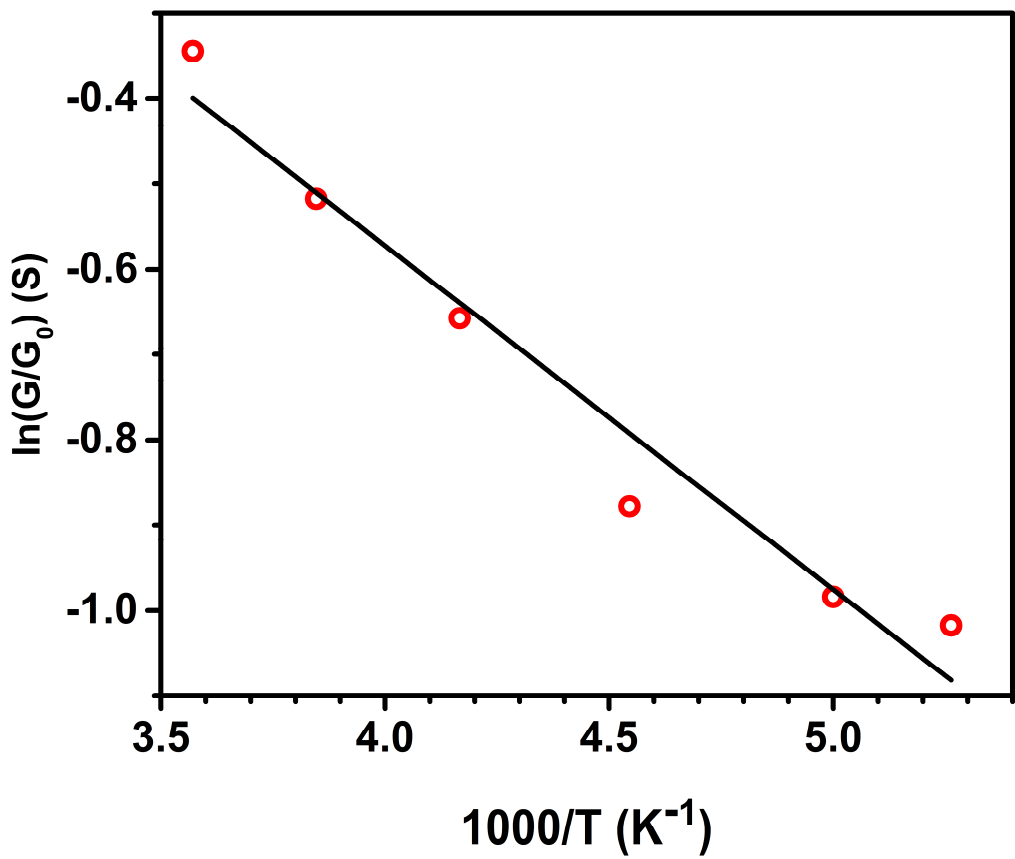


Figure S15: Linear fit to high temperature region of the variable temperature electrical conductivity plot shown in Figure S14.

Mössbauer Spectroscopy

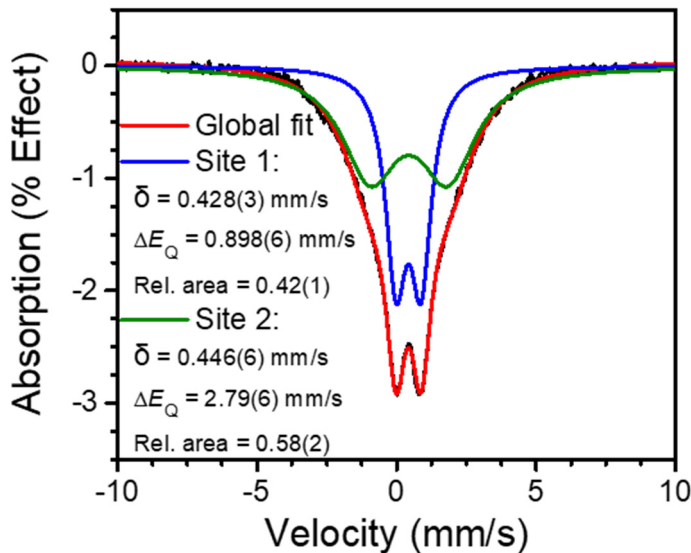


Figure S16: ^{57}Fe Mössbauer spectrum of **1-Li** collected at 80 K with fit to a two site model.

Table S2: Mössbauer fitting parameters.

Parameter	Site 1	Site 2
Isomer shift (δ)	0.428(3) mm/s	0.446(4) mm/s
Quadrupole splitting (ΔE_Q)	0.898(6) mm/s	2.79(6) mm/s
Relative area	0.42(1)	0.58(2) mm/s
Gaussian broadening, FWHM	0.90(2) mm/s	2.43(3) mm/s

IR Spectroscopy

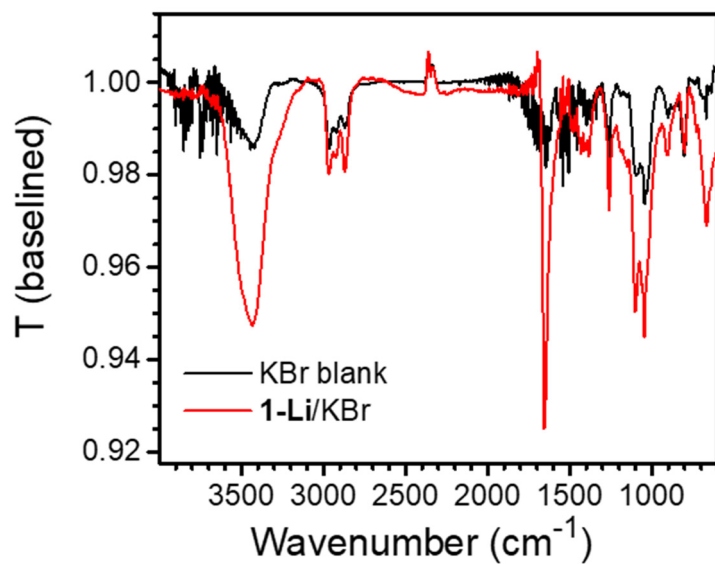


Figure S17: FTIR spectrum of **1-Li** prepared as a KBr pellet.

Electrochemical Measurements

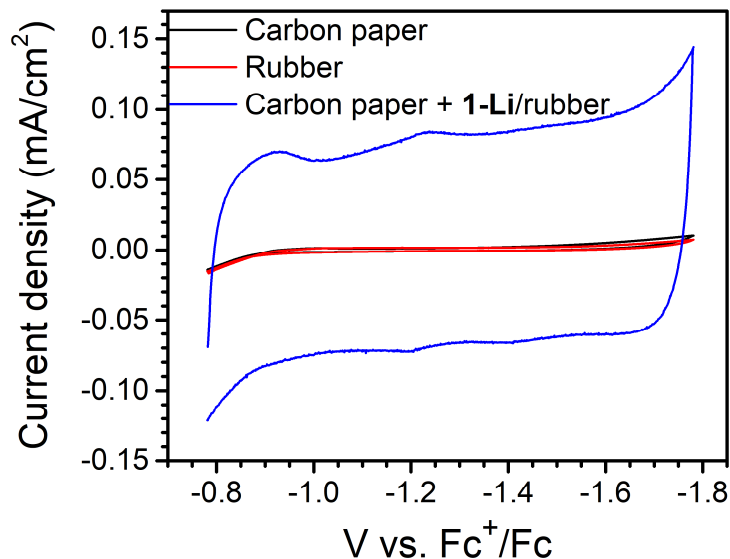


Figure S18. Cyclic voltammograms (1 mV/s, 0.1 M LiCF₃SO₃ in DMF) of carbon paper electrode coated with **1-Li** + 10% rubber slurry and control electrodes. Current densities are calculated using the geometric areas of the electrodes (2 cm²).

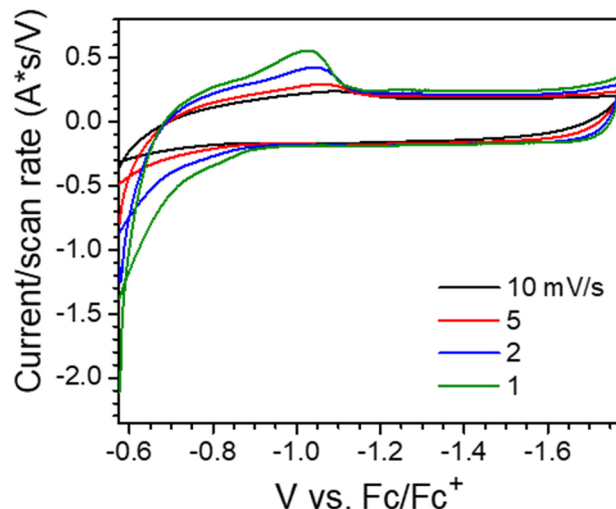


Figure S19: Cyclic voltammetry data for **1-Li** composite electrode in 0.1 M LiCF₃SO₃/DMF showing Faradaic features. Data is plotted as current/scan rate, which for a capacitor gives the capacitance in Farads. Pseudocapacitive features should show no scan rate dependence, while Faradaic features should decrease at higher scan rates.

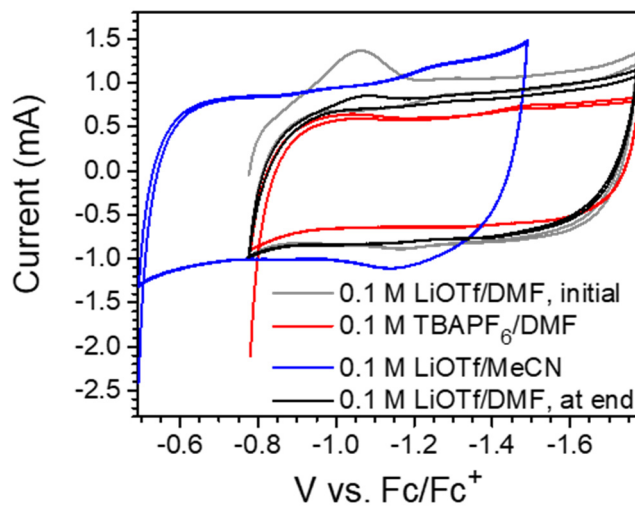


Figure S20: Cyclic voltammograms of the same **1-Li** composite electrode in different electrolytes, measured at 10 mV/s. LiOTf = LiCF₃SO₃.

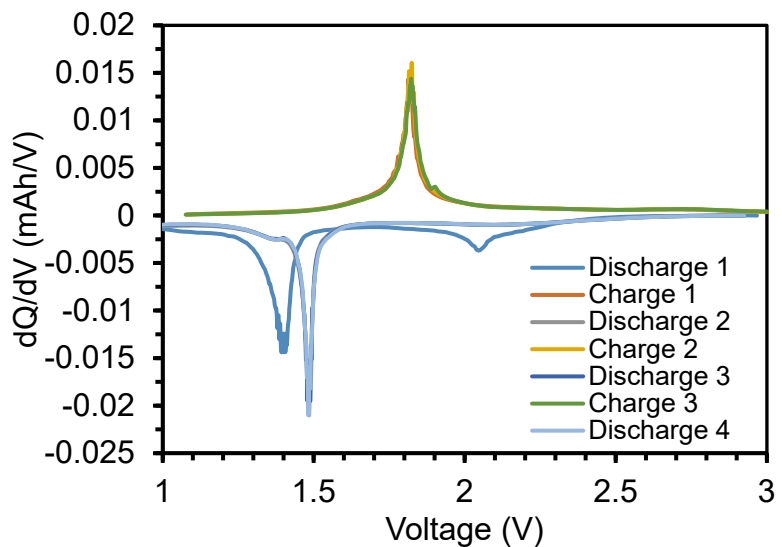


Figure S21: dQ/dV plot for 1-Li lithium ion cathode half cell tests at 0.1C.

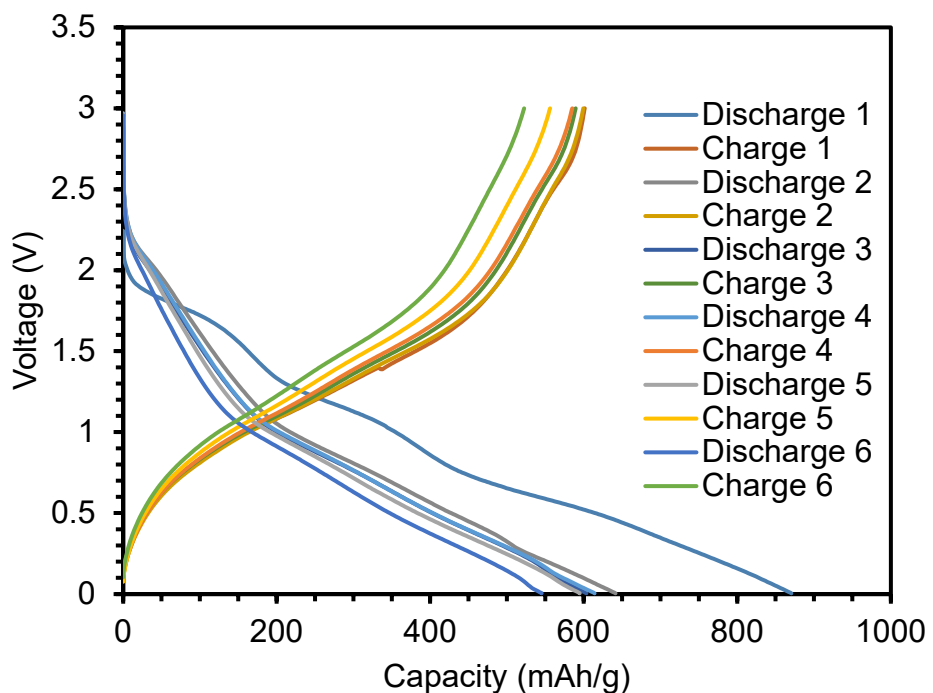


Figure S22: Charge/discharge curves for 1-Li sodium ion cathode half cell tests. V = 0.005 – 3.0 V vs. Na, I = 30 mA/g, 1M NaPF₆ in EC/DEC + 2w% FEC.

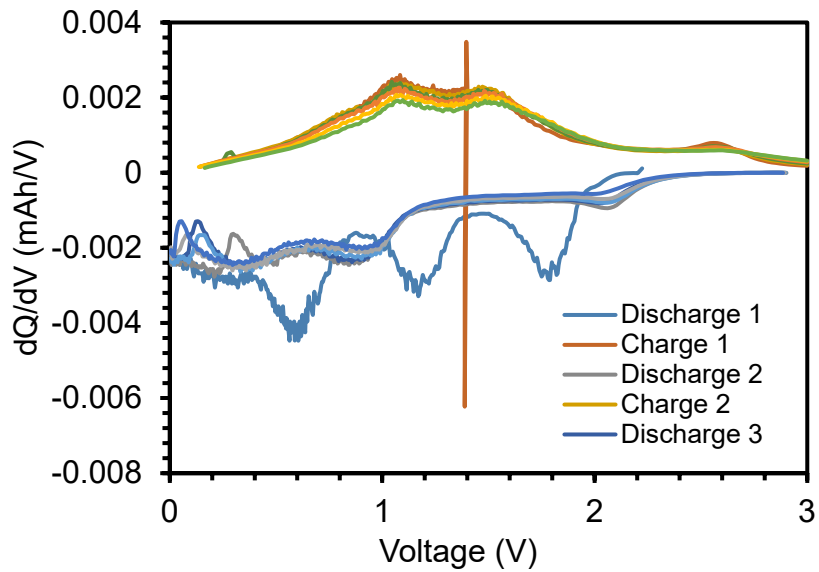


Figure S23: dQ/dV plot for 1-Li sodium ion cathode half cell tests.

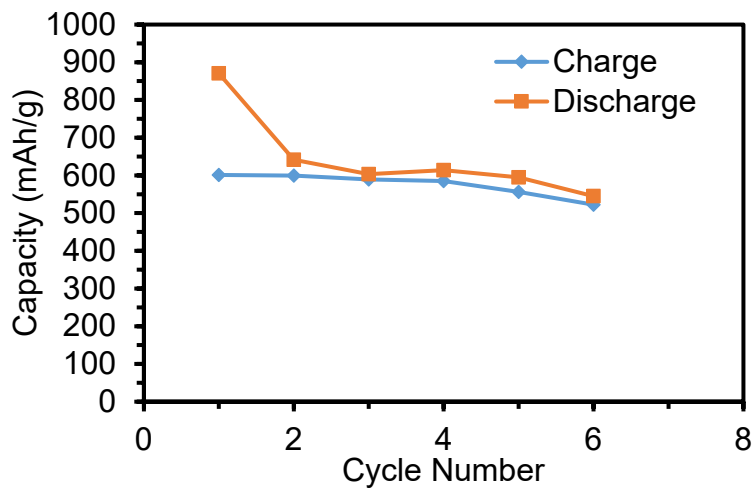


Figure S24: Cycling stability of 1-Li sodium ion cathode in half cell tests.